Superplastic HSLA Steels: Microstructure and Failure

Sara Fernandez, María José Quintana, José Ovidio García, Luis Felipe Verdeja, Roberto González & José Ignacio Verdeja

Journal of Failure Analysis and Prevention

ISSN 1547-7029

J Fail. Anal. and Preven.
DOI 10.1007/s11668-013-9662-9

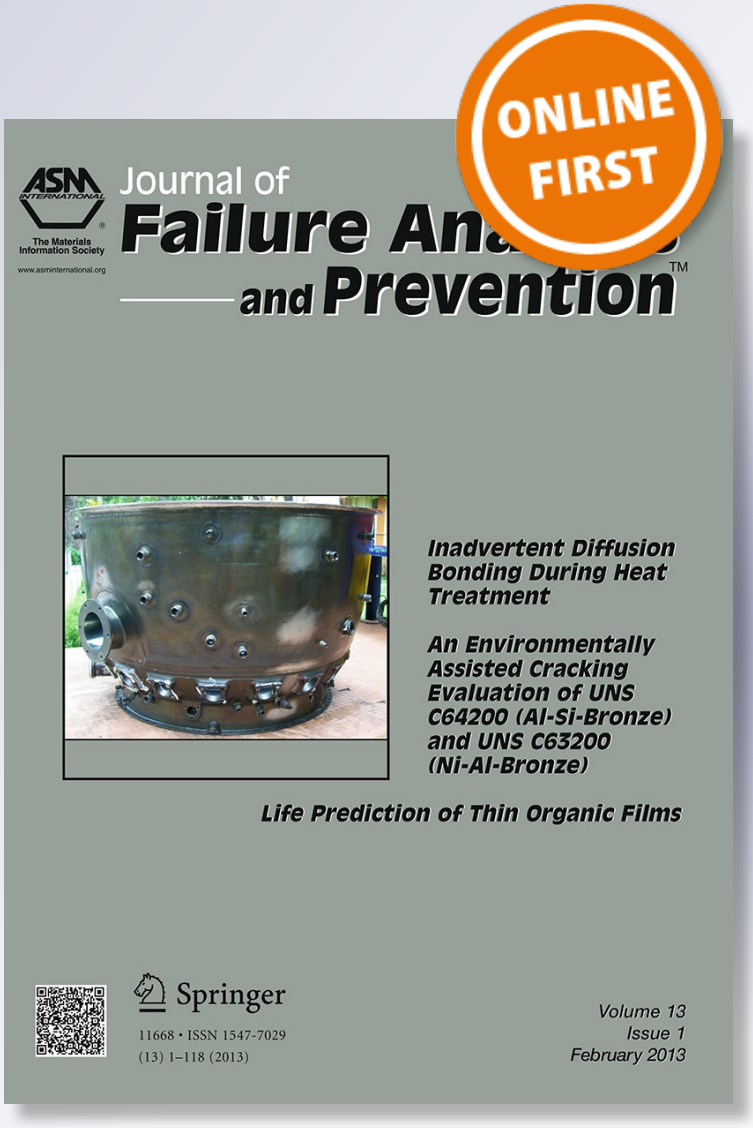

Springer

J Fail. Anal. and Preven.
DOI 10.1007/s11668-013-9662-9

TECHNICAL ARTICLE—PEER-REVIEWED

Superplastic HSLA Steels: Microstructure and Failure

Sara Fernandez · María José Quintana · José Ovidio García · Luis Felipe Verdeja · Roberto González · José Ignacio Verdeja

Submitted: 16 October 2012

Abstract Certain materials can show superplasticity when traction tested at temperatures higher than 50% of their melting point and with low strain rates ($\dot{\varepsilon} < 10^{-2}$ s^{-1}), showing very high elongations (>100%) without localized necking and mainly intergranular fractures. This behavior requires that the starting grain size is small (<10 μm) so the flow of matter can be non-homogeneous (sliding and rotating of the grain boundaries, accommodated by diffusion). This work presents the superplastic characteristic of shipbuilding steel deformed at 800 °C and a strain rate slower than 10^{-3} s^{-1}. The fine grain size (5 μm) is obtained when using Nb as a microalloying element and manufactured by controlled rolling processes (three stages). After the superplastic deformation, the steel presents mixed fractures: by decohesion of the hard (pearlite and carbides) and ductile (ferrite) phases and by intergranular sliding of ferrite/ferrite and ferrite/pearlite, just as it happens in stage III of the creep behavior. This is confirmed through the Ashby–Verrall model, according to which the dislocation creep (power-law creep) and diffusion creep (linear-viscous creep) occur simultaneously.

Keywords Superplasticity · Ultrafine grained · Strain rate *m* coefficient · Boundary sliding · High-strength low-alloy steels (HSLA steels)

This article is an invited paper selected from presentations at the Microscopy & Microanalysis 2012 Annual Meeting, held July 29–August 2, 2012, in Phoenix, Arizona, and has been expanded from the original presentation.

S. Fernandez · J. O. García · L. F. Verdeja · J. I. Verdeja
E.T.S.I.M.O., Universidad de Oviedo, Independencia 13, 33004 Oviedo, Spain

L. F. Verdeja
e-mail: lfv@etsimo.uniovi.es

M. J. Quintana (✉) · R. González
School of Engineering, Universidad Panamericana, Augusto Rodin 498, 03920 Mexico, DF, Mexico
e-mail: mquintana@up.edu.mx

R. González
e-mail: robglez@up.edu.mx

Introduction

A material is considered to have superplastic behavior when it shows extremely high and uniform elongations (from 100 to 1000%) under tension stress: a lack of localized necking or a series of diffuse necks along the test zone resulting from a combination of the creep tension stress and the strain rate suffered by the polycrystalline arrangement [1]. Two mechanisms are considered to take place in the material: grain boundary migration and grain boundary shearing/sliding. Theoretic and microstructural models agree that the most important feature of this behavior is the grain boundary sliding (GBS). Nevertheless, dislocations or diffusion in grains or in zones near grain boundaries are necessary in order to maintain the continuity of the material (and avoid ductile decohesions) [2].

Four conditions must be met [3] in order for a material to show superplasticity:

- a stable microstructure of fine equiaxed grains [4],
- *m* coefficient (strain rate sensitivity exponent; $\sigma = K\dot{\varepsilon}^m$) values between 0.3 and 0.7,
- slow strain rates (10^{-3}–10^{-5} s^{-1}), and
- grain boundaries of the material that allow grain sliding and rotation when stress is applied [5].

In addition to the previous requirements, it is necessary to deform the material at the right temperature, which is a

Published online: 06 February 2013

fundamental characteristic in some superplastic behavior models, such as the one established by Ashby and Verrall [6]. Their model proposes a theory (Grain Boundary Sliding, Diffusion-Accommodated Flow Rate Controlling) to describe superplasticity, taking into account two mechanisms:

(a) the diffusion-accommodated flow (D-A flow) consisting of GBS along with material transport through the grain boundary and bulk crystal diffusion [7] to maintain grain continuity (this phenomena dominates in the low stress regime, strain rates lower than 10^{-5} s^{-1}) and
(b) the ordinary power-law creep (dislocation creep) which is a quasi-uniform flow mechanism that results in grain elongation as dislocations accumulate as cells, storing energy; this last mechanism dominates at sufficient high stresses (strain rates higher than 10^{-3} s^{-1}). In the intermediate stress range, both mechanisms compete in order to achieve the superplastic behavior.

The work presents the high temperature superplastic behavior of an ultrafine-grained steel (UFG) microalloyed with Ti–Nb obtained by advanced thermomechanical control rolling processes (ATMCRP), at the Arcelor Mittal factory in Veriña (Gijón, Spain), as materials of this type can show this behavior when certain conditions are met. The characteristics of the steel, delivered in the form of 27.6-mm-thick sheets (around one inch), are described in the experimental procedure. The HSLA steels described in Euronorms 10149-2 and 10051 are examples of these materials as well as other construction steels or automotive special steels (just as the ones described in the ultralight steel auto body—ULSAB project), resulting in lower cost materials and a step forward in the research for better materials in industry, such as lightweight structures and components with very good weldability which are easier to recycle; all of this reduces the cost of the alloy and meets high specifications with steels that have a lower amount of alloying elements and that are considered high-tech [8]. Furthermore, UFG may be applied in the future in most of the steel markets and can be used in other industrial applications, such as the ones that require superplastic behavior, just as this work demonstrates.

UFGs (grain size $\bar{d} = 1$–5 μm) are currently intensively studied worldwide as they offer a solution to finding very high strength materials. They also present high toughness and are produced from standard steel compositions (which reflects in low cost) [9]. Recent works have shown that the ultrafine-grained structure may be obtained in a hot rolling mill by ATMCRP and not just from small-scale laboratory tests [4, 10]. However, under some circumstances, these materials may present an important disadvantage as they exhibit unstable plasticity upon yielding, severely restricting their potential uses [11]. In order to avoid this instability [12], the mechanical behavior of the steel must show a strain hardening coefficient n (as measured by a tension test with the ASTM standard) higher than 0.1 in its hot rolling raw state. If this is achieved, the steel can be used for cold work operations such as bending, stretching, and drawing and in commercial applications such as automotive and other manufacturing industries [4]. Also, in order for the superplastic behavior to show, high strain rate sensitivity, high temperature testing ($>1/2T_m$), a fine microstructure, and a relatively low strain rate are required [13–15].

As an ultrafine-grained microstructure is essential to obtain a superplastic behavior, the steel was produced by ATMCRP, which manly consists of three steps:

- roughing (in order to reduce the thickness of the slab),
- delay time (where the material is cooled between 1000 and 850 °C) to obtain Ti and Nb carbides, and
- finishing (where the deformation is accumulated in the austenite in order to obtain the finest ferrite possible after the allotropic transformation), in the same fashion as described in previous work [10].

In order to achieve this small grain size microstructure, the composition of the steels is very important. Figure 1 shows the changes in grain size during the roughing process for both a steel sample microalloyed with Nb and one without it. It is clear that the alloying element promotes a smaller grain size and prevents growth after rolling passes. On the other hand, Fig. 2 compares the recrystallization kinetics (amount of recrystallized grains) of steels with and without Nb, showing that the microalloying element delays the recrystallization process and allows the production of steels with smaller (ultrafine) grains [16].

Experimental Procedure and Results

The specified chemical composition for this steel (in wt.%) according to the Euronorm is as follows: C 0.168, Mn 1.361, Si 0.453, P 0.022, S 0.009, Cu 0.026, As 0.003, Al 0.028, Cr 0.035, *Ti 0.026*, V 0.002, *Nb 0.033*, Mo 0.004, Ni 0.031, Sn 0.002, Al (soluble) 0.027, B 0.0001, N 0.0055, Zr 0.0000, Ca 0.0001, O 0.0000, H 2.00 ppm, B (soluble) 0.0000. In the same way, the specified mechanical properties are higher yield stress (σ_y) = 447 MPa, ultimate tensile stress (σ_{max}) = 567 MPa, yield elongation with L_0 of 50 mm (El) = 31%, and impact resistance at −20 °C (KCV) = 96 J.

The samples were obtained from the steel sheet in an axis parallel to rolling direction and were machined in a cylindrical shape: 10 mm in diameter and calibrated gage

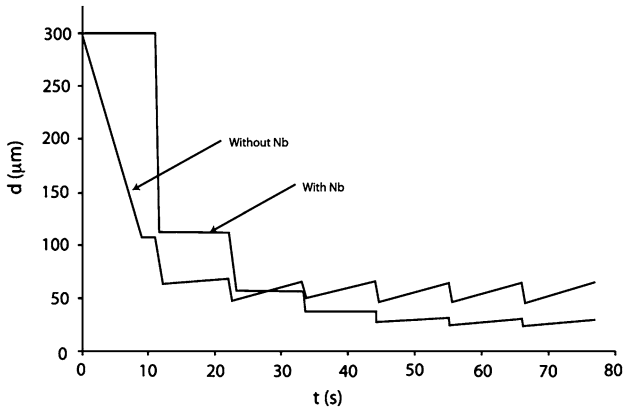

Fig. 1 Grain size versus time in the roughing process of steels with and without Nb

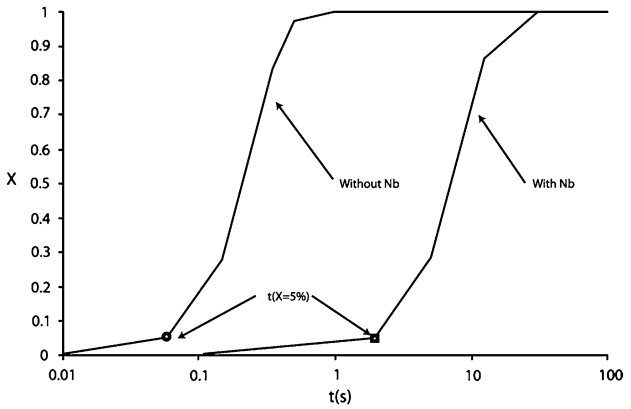

Fig. 2 Evolution of recrystallization kinetics during the finishing passes of steels with and without Nb

length of either $L_0 = 57$ or $L_0 = 30$ mm (ASTM E21-05 standard). High temperature tension tests were conducted at different temperatures between 600 and 900 °C (50 °C intervals) and different crosshead speeds in order to define the temperature interval at which the steel would show a superplastic behavior. After defining a temperature in which the material presented this characteristic, more tests were conducted using different crosshead speeds in order to determine the optimum strain rate at which the steel behaves superplastically. An INSTRON 1195 model equipment for traction test with a load capacity of 100 kN was used along with an INSTRON 3112 model furnace which allows reaching temperatures as high as 1000 °C. The tests were conducted without a protective atmosphere at speeds between 0.05 and 10 mm/min (strain rates in the range of 10^{-3}–10^{5} s^{-1}). Before the tests were performed, uniform heating from room to test temperature was conducted, lasting 1 h, followed by 5–10 min of stabilization. Variations of temperature inside the furnace were of maximum ±10 °C.

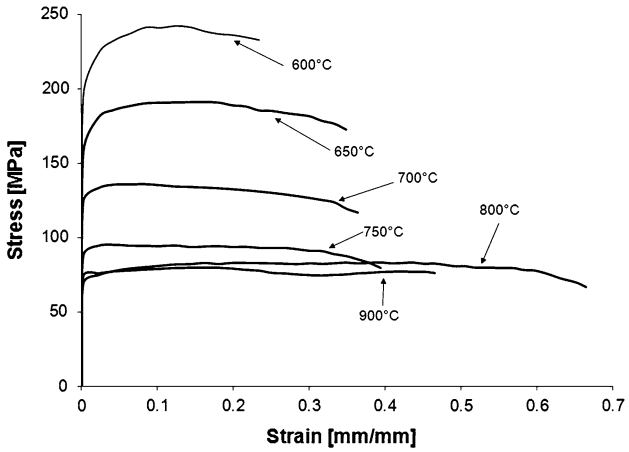

Fig. 3 True stress–strain curves at different temperatures and 5 mm/min crosshead speed ($L_0 = 57$ mm)

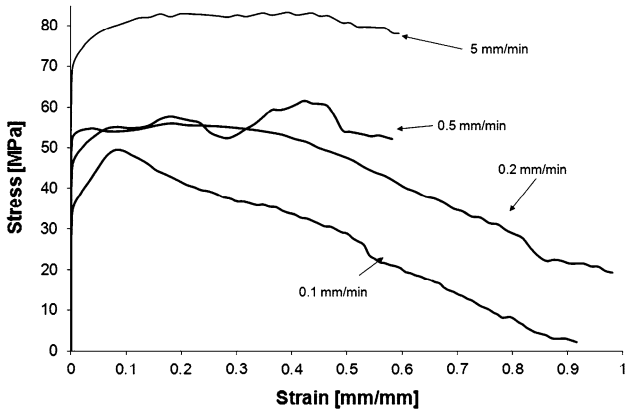

Fig. 4 Engineering stress–strain curves at 800 °C and different crosshead speeds

Figure 3 presents the true tensile curves for samples tested at six different temperatures and a crosshead speed of 5 mm/min. As expected, the higher the temperature, the lower the maximum stress the sample may withstand, which for 600 °C is above 200 MPa and for 900 °C is below 80 MPa. It is noteworthy that at 800 °C, the steel shows the highest value for the true strain (~0.7) and almost steady state regime, like in secondary creep (which is an indication of superplasticity) [17].

Once 800 °C was determined as a temperature at which the material may present superplastic behavior, tensile tests at different crosshead speeds were conducted with this temperature value (Fig. 4). Though some ripples are evident during deformation at 5 mm/min, this phenomenon is increased at 0.5 mm/min. The smooth deformation of the samples is only achieved when the crosshead speed is lowered to 0.2 mm/min. For 0.2 and 0.1 mm/min, the true strain of the samples is close to 100%. Table 1 presents the results obtained from the tensile tests conducted at 800 °C

Table 1 Tests conducted at 800 °C using different strain rates

	L_0 (mm)	V_t (mm/min)	σ_y (MPa)	A (%)	$\dot{\varepsilon}$ (s^{-1})	Log ($\dot{\varepsilon}$)	Log (σ_y)
Non-superplastic tests	57	5	70.0	>109.2	1.46E−03	−2.84	1.845
	30	0.5	57.3	92.7	2.78E−04	−3.56	1.758
	57	0.5	45.8	>111.4	1.46E−04	−3.84	1.660
Superplastic tests	30	0.2	52.8	191.3	1.10E−04	−3.96	1.723
	57	0.2	37.6	>110.0	5.85E−05	−4.23	1.575
	30	0.1	34.4	181.7	5.56E−05	−4.25	1.237
	30	0.05	27.4	137.5	2.78E−05	−4.56	1.438

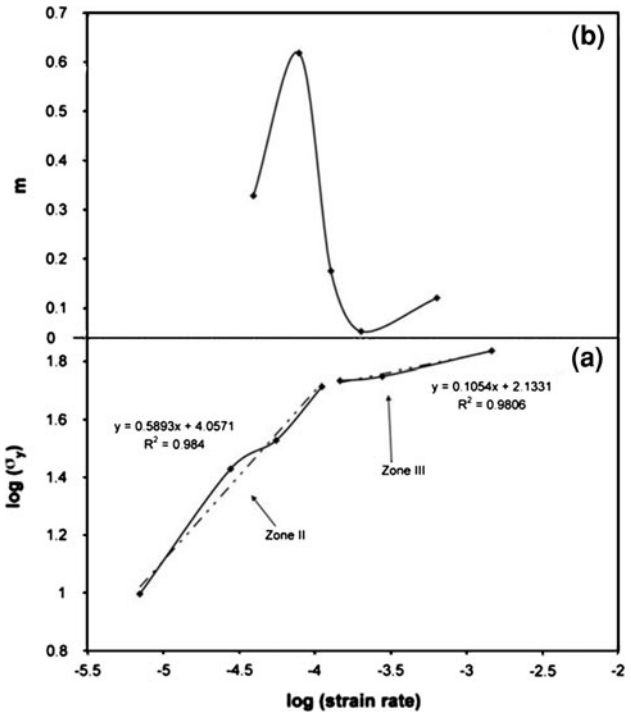

Fig. 5 Influence of strain rate on yield stress (**a**) and super-index m (**b**) in superplastic behavior at 800 °C

at different strain rates and different types of tests (tension and superplastic tests).

Considering the expression $\sigma = K\dot{\varepsilon}^m$ (where K is a function of the temperature), the previous deformation the steel may have suffered and the grain size, coefficient m expresses the sensitivity of the applied tension to strain rate as follows:

$$m = \left(\frac{\log(\sigma_{y_2}/\sigma_{y_1})}{\log(\dot{\varepsilon}_{0_2}/\dot{\varepsilon}_{0_1})}\right)_{T,d,\varepsilon} \quad \text{(Eq 1)}$$

with σ_y and $\dot{\varepsilon}_0$ being the yield stress at 0.2% and the initial strain rate, respectively, in tests conducted at two different strain rates. Figure 5 presents the logarithm of yield stress versus the logarithm of strain rate, where two different slopes of the data may be identified as zone II and zone III behaviors of the typical sigmoidal high temperature curve [7]. Also, Fig. 5b presents the values of the m coefficient with a maximum of $\sim$0.6, which is in the superplastic range, for a strain rate of $\sim 5.5 \times 10^{-5}$ s^{-1}.

Metallographic observations were carried out before and after the high temperature tests were conducted, analyzing the transverse sections of the samples in an axis parallel to the rolling direction. For most of the samples, normal grinding, polishing, and etching procedures with Nital-2 solution were used. A Nikon Epiphot metallographic equipment connected to a Buehler Omnimet image analyzer, which allows the automated counting of features using linear intersection techniques and point counting over a mesh superposed to the microstructure image at ×400 and ×600, was used in the analysis in order to determine the ASTM grain size and its distribution of the ferrite grains. A sufficient amount of micrographs (a minimum of 5) was used during counting. The metallographic observation was also used to analyze different types of structural damages produced during superplastic deformation of selected samples. A scanning electron microscope (SEM) JEOL JSM-5600 with an electroprobe analyzer OXFORD model 6587 was used to observe characteristics such as decohesions and identify small precipitates.

The microstructural analysis of the ferrite grains in the steel in its raw state (Fig. 6), along with the analysis of grain size distribution, shows a 13 ASTM G grain size mean value, which corresponds to approximately 5 μm. This value is small enough for the material to show, under the proper conditions of temperature and strain rate, superplastic behavior. It is also evident from Fig. 6 that the hot rolling direction (horizontal axis) produces ferrite and pearlite bands and oriented microstructure.

Figure 7 shows the microstructure of a sample after being superplastically deformed at 800 °C (0.1 mm/min crosshead speed) at a zone 15 mm from the rupture of the specimen. The banded oriented structure has almost disappeared and restored ferrite grains are observed. Also, Fig. 8 shows characteristics of the structure at the same zone with evidence of decohesion between the ferrite and/or the ferrite–pearlite grains of different types. These is evidence of superplastic mechanisms acting during deformation of the sample [18].

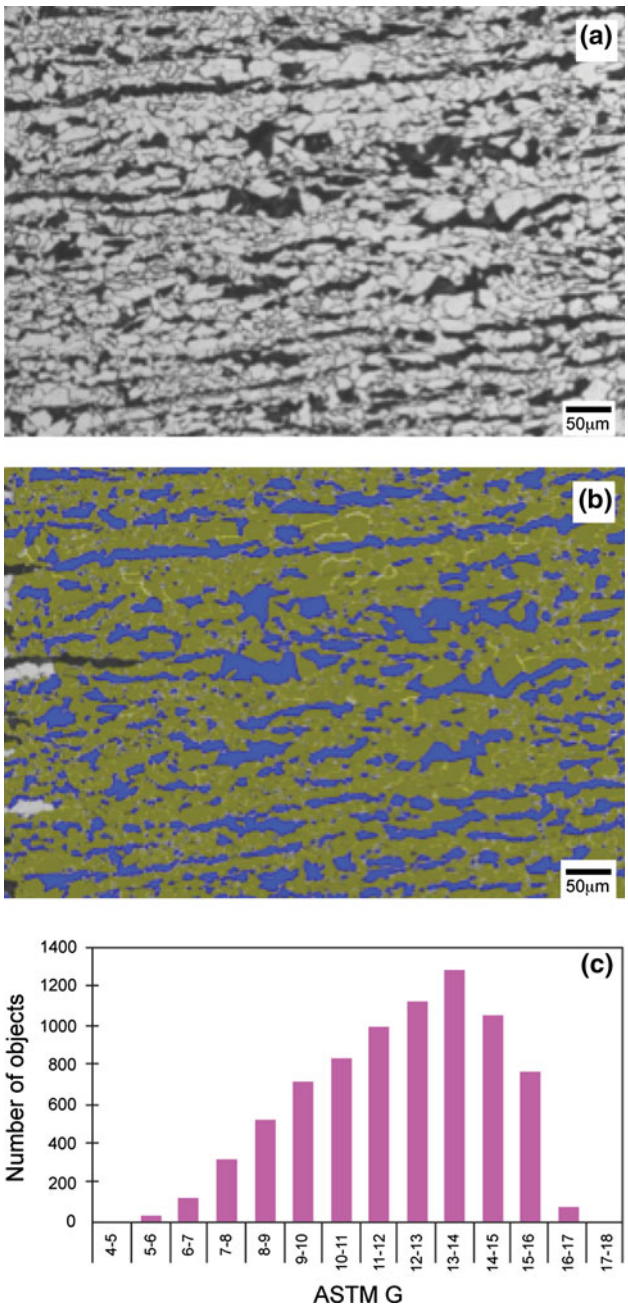

Fig. 6 Hot-rolled raw state microstructure (**a**), detected ferrite grain pattern (**b**), and ASTM G grain size distribution histogram (**c**)

Discussion

The microstructure of the steel shown in Fig. 6 is formed by ferrite and pearlite bands, typical in construction steels which have suffered a peritectic reaction and solidification under non-equilibrium conditions. As the partition coefficient for carbon, alloying elements (Mn and Si), and impurities (P, S) in this steel is lower than one, the microstructure cannot be regenerated during soaking treatment before hot rolling [19].

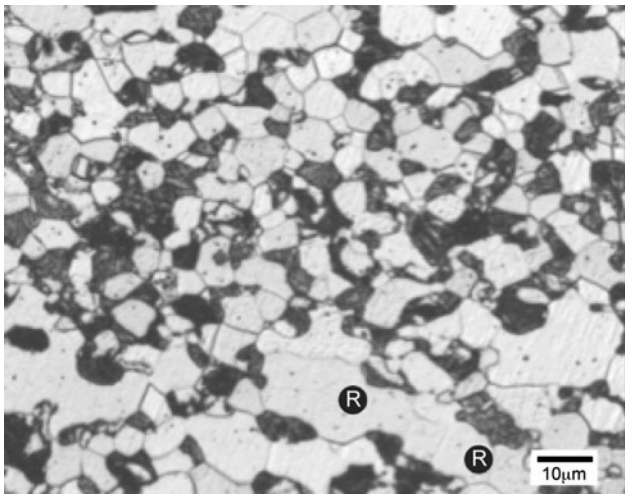

Fig. 7 Micrograph of a specimen superplastically deformed at 800 °C at a zone close to rupture (15 mm away from it). Restored ferrite (*R*) is observed

In the initial microstructure, both ferrite and pearlite grains are continuous and elongated in the rolling direction, while the ferritic volume fraction is higher than the pearlitic one, which is ~30%.

If the original banded microstructure is compared to the one of the sample tested at 800 °C and 0.1 mm/min (Fig. 9a, b), it is clear that the bands have not completely disappeared though the ferrite phase has suffered restoration without a significant grain size enlargement. If these two microstructures are compared to the sample tested at 750 °C and 0.1 mm/min (Fig. 9c), a clear difference can be observed as testing at a lower temperature results in a complete disappearance of the pearlitic bands, being replaced by ferrite grains and precipitates (mostly carbides).

Figure 7 presents after deformation ferrite grains of a larger size which are slightly elongated in the rolling direction with evidence (subgrains) of having suffered dynamic recovery during deformation. Furthermore, Fig. 8 shows the following:

- decohesions shaped as w and r, mainly located in the ferrite/pearlite (previous austenite grains) interphase, which is an unequivocal proof of intergranular sliding during the deformation process.
- small cavities in the α-pearlite (previous austenite grains) interphase, which shows a different deformation capacity for each of these phases.
- null evidence of generalized grain growth during deformation as grain size is very similar (or even slightly smaller, <5 μm) to the original one.
- grain (or grain groups) sliding and rotating, a consequence of superplastic deformation.

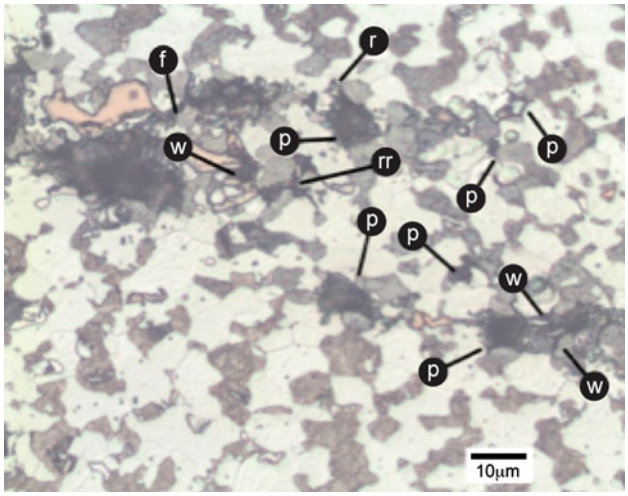

Fig. 8 Micrograph of a specimen superplastically deformed at 800 °C at a zone close to rupture (15 mm away from it). W-shaped decohesion between ferrite–ferrite–pearlite (*w*), r–r-shaped decohesion between ferrite and pearlite (*rr*), ferrite–pearlite decohesion (*f*), and ferrite–ferrite (*r*) or pearlite–pearlite decohesion (*p*) are observed

Figure 10 shows evidence of decohesions which are the evidence of superplastic behavior in the steel and consequence of the grain sliding. Also, Fig. 11 shows another type of decohesion resulting from boundary sliding of three grains (one grain displaces the other two).

Furthermore, decohesions between ferrite and pearlite may result in cavities with evidence of ductile deformation of the softer phase, as shown in Fig. 12. Superplastic flow stops when the intergranular damage and decohesions between the matrix and inclusions lead to ductile fracture.

The importance of decohesions is evident if the role of Ti and Nb carbides (or carbonitrides) is taken into account as these particles are not dissolved during the 800 °C test (Fig. 12): These precipitates anchor the grain boundary and prevent recrystallization and grain growth during rolling at the finishing stage, which is accompanied by the formation of γ-pancaked grains and deformation bands. Consequently, a larger number of nucleation sites are made available for the $\gamma \rightarrow \alpha$ transformation. This allows the formation of an ultrafine microstructure, fulfilling the requirements for both strength and toughness [20, 21].

The initial composition (Nb and Ti content) of the steel and the evidence of an ultrafine microstructure after ATMCRP indicate that the role of NbC and Ti(C,N) is very important during both room temperature and high temperature deformation of the material. Figure 13 shows a particle precipitated at grain boundaries, which was initially formed as a titanium carbonitride and then became a substrate for a niobium carbide layer, as confirmed by other authors [20].

If at a lower magnification, precipitates are observed (Fig. 14), it is evident that most of the titanium carbonitrides grow along the former pearlite bands, and as previously mentioned, the niobium carbides appear at the same spots using the titanium precipitates as a substrate.

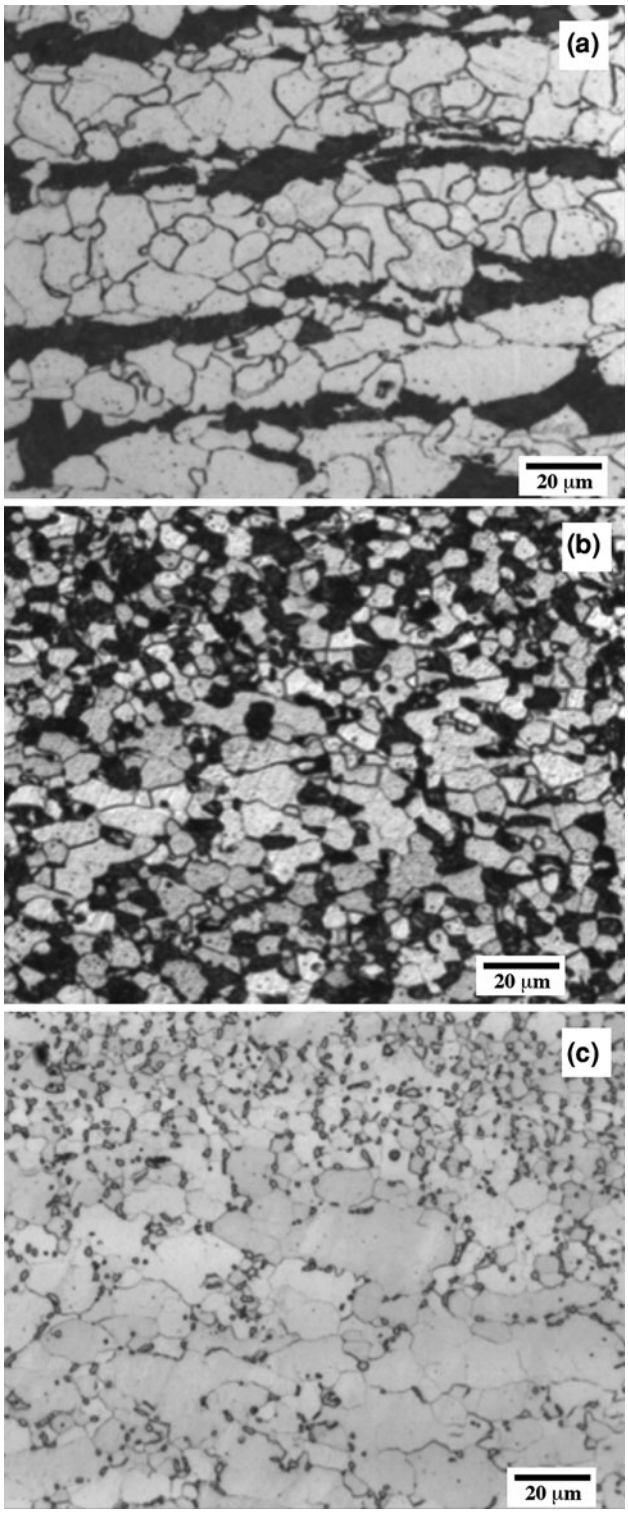

Fig. 9 Microstructure of the steel in its hot-rolled raw state (**a**), tested at 800 °C and 0.1 mm/min crosshead speed (**b**), and tested at 750 °C and 0.1 mm/min crosshead speed (**c**)

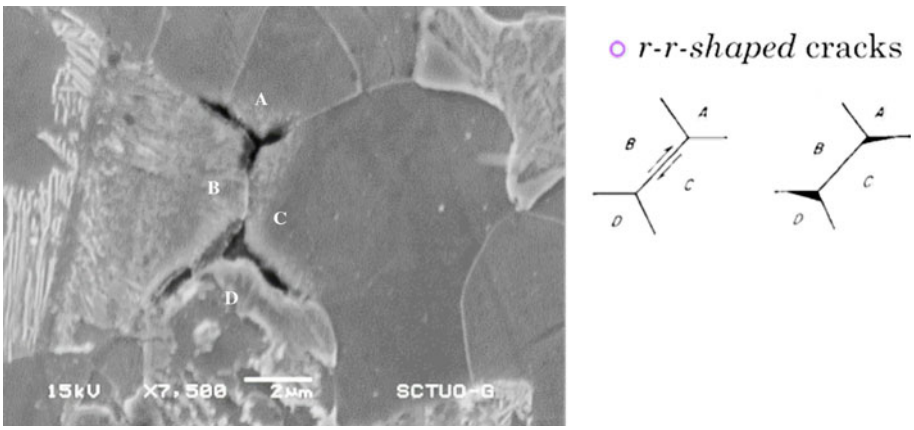

Fig. 10 SEM micrograph of the steel tested at 800 °C showing a r–r-shaped decohesion

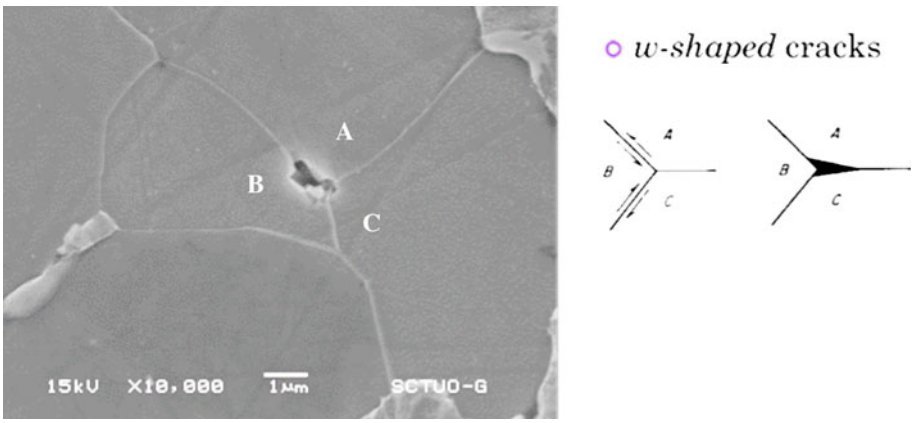

Fig. 11 SEM micrograph of the steel tested at 800 °C showing a w-shaped decohesion

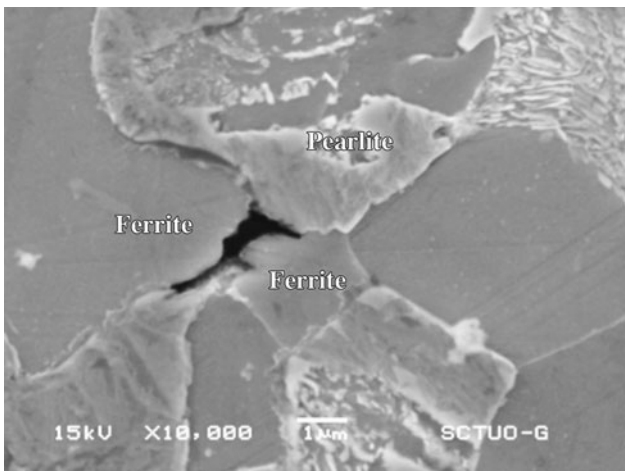

Fig. 12 SEM micrograph of the steel tested at 800 °C showing a ferrite–pearlite (ductile) decohesion

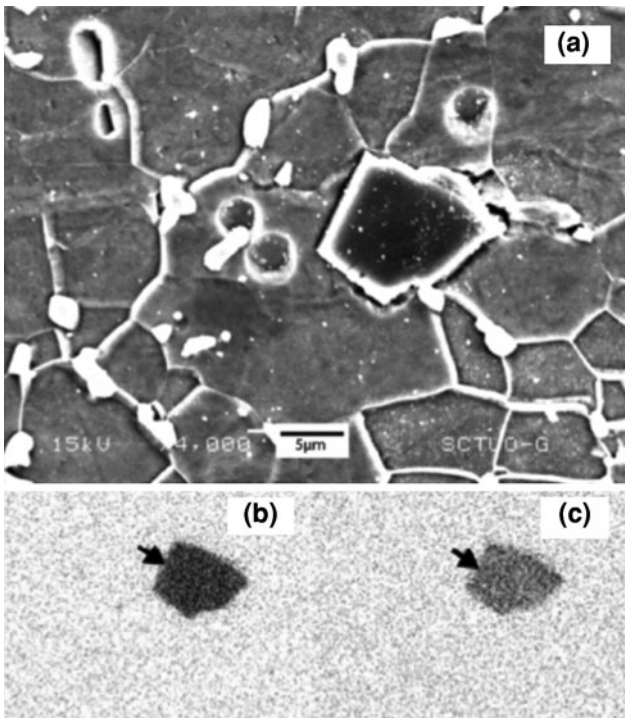

Fig. 13 SEM micrograph showing a titanium carbonitride and niobium carbide (**a**), dot mapping of titanium (**b**), and dot mapping of niobium (**b**)

Figure 15 presents curves of the Ashby–Verrall model for a metallic polycrystalline arrangement for grain sizes of 1, 5, and 10 µm. The use of the σ/μ ratio, where μ is the shear modulus, allows the comparison of the experimental data with models for an arrangement of polycrystalline

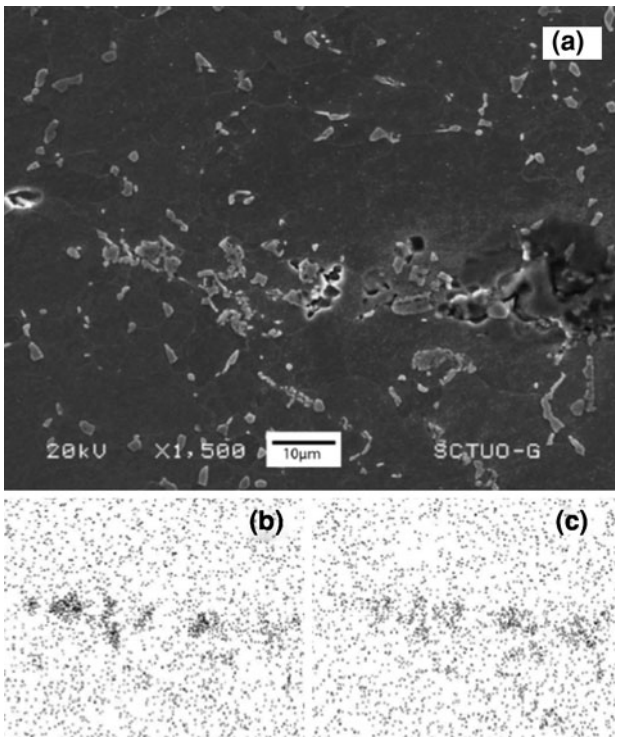

Fig. 14 SEM micrograph showing a string of titanium carbonitrides and niobium carbides (**a**), dot mapping of titanium (**b**), and dot mapping of niobium (**c**)

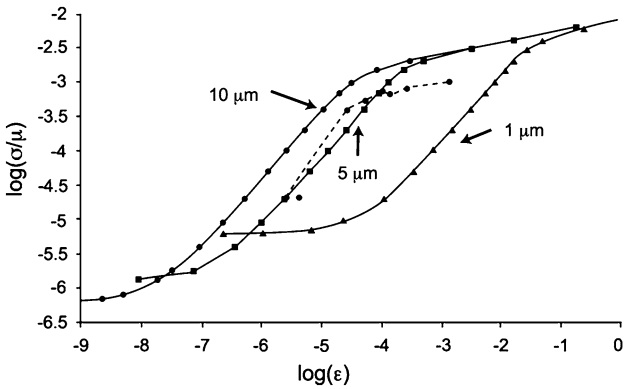

Fig. 15 Theoretic curves (Ashby–Verrall model) of logarithm of yield stress/shear modulus versus logarithm of strain rate considering different grain sizes as well as for the steel investigated (*dashed line*)

metallic materials and where μ ($\sim$70 GPa at 800 °C in this steel) is a function of the testing temperature [6]. The dashed line indicates the values obtained from the high temperature tests of this steel, which lie very close to the 5 μm curve, though with lower amplitude. This behavior may be explained as a reduction in yield stress caused by the banded structure, even though grains are of the ultrafine type. Consequently, the Ashby–Verrall model seems to be an appropriate description of the relations between temperature, yield stress, strain rate, and grain size of the mechanical behavior of this steel.

Conclusions

Commercial weldable HSLA steels microalloyed with Ti/Nb and obtained by ATMCRP present ultrafine-grained microstructures and superplastic behavior (elongations higher than 100%) when deformed in the ferrite–austenite region at 800 °C with strain rates close to 5×10^{-5} s^{-1}.

The microstructural analysis of decohesions at the steel after testing confirms the grain sliding phenomena described by the model and is also clear evidence of superplasticity. The role of precipitates is not limited to the formation of ultrafine microstructure during ATMCRP, but is also very important during high temperature tests as they prevent grain growth and maintain mechanical strength acting as grain boundary dislocation barriers.

The Ashby–Verrall model is suitable to describe the superplastic behavior of the steel. The most important feature of this model is the GBS and rotation along with bulk crystal diffusion to maintain the continuity of the steel.

Acknowledgments The authors thank the Department of Metal Sheet and Hot Coil of Mittal Arcelor of Gijón–Avilés (Asturias, Spain) for providing samples for this research. Also, thanks to T. Iglesias and B. Mendieta for the preparation of images and figures.

References

1. Backofen, W.A., Turner, I.R., Avery, H.: Superplasticity in an Al–Zn alloy. Trans. ASM **57**, 980–990 (1964)
2. Sherby, O.D., Wadsworth, J., Oyama, T.: Superplasticity: Prerequisites and Phenomenology. Universidad Politécnica de Madrid E.T.S.I.C.C.P., Madrid (1985)
3. Alden, T.H.: Plastic Deformation of Materials. Review Topics in Superplasticity, pp. 225–266. Academic Press, New York (1975)
4. González, R., García, J.O., Barbés, M.A., Quintana, M.J., Verdeja, L.F., Verdeja, J.I.: Ultrafine grained HSLA steels for cold forming. J. Iron Steel Res. Int. **17**(10), 50–56 (2010)
5. Avery, D.H., Backofen, W.A.: Trans. ASM **58**, 551–562 (1965)
6. Ashby, M.F., Verrall, R.A.: Diffusion-accommodated flow and superplasticity. Acta Metall. Mater. **21**, 149 (1973)
7. Pero-Sanz, J.A.: Science and Materials Engineering. CIE–Dossat 2000, Madrid (2006) (in Spanish)
8. Broek, C.T.: FutureSteelVehicle: leading edge innovation for steel body structures. Ironmak. Steelmak. **39**(7), 477–482 (2012)
9. Mukherjee, K., Hazra, S.S., Militzer, M.: Grain refinement in dual-phase steels. Metall. Mater. Trans. A **40A**, 2145–2159 (2009)
10. Quintana, M.J., Gonzalez, R., Verdeja, L.F., Verdeja, J.I.: Dual-phase ultrafine-grained steels produced by controlled rolling processes. In: Materials Science and Technology (MS&T), Columbus, 16–20 Oct 2011, p. 504
11. Howe, A.A.: Ultrafine grained steels: industrial prospects. Mater. Sci. Technol. Ser. **16**, 1264–1266 (2000)

12. Gonzalez, R., Quintana, M.J., Verdeja, L.F., Verdeja, J.I.: Ultrafine grained steels and the *n* coefficient of strain hardening. Mem. Trab. Difus. Cient. Tec. **9**, 45–54 (2011)
13. Morrison, W.B.: Superplasticity of low-alloy steels. Trans. ASM **61**, 423–434 (1968)
14. Reed-Hill, R.E.: Creep. In: Physical Metallurgy Principles, 2nd edn, pp. 827–887. D. Van Nostrand Company, New York (1973)
15. Vetrano, J.S.: Superplasticity: mechanisms and applications. JOM **3**, 22 (2001)
16. Capdevila, C., Amigo, V., Caballero, F.G., García de Andres, C., Salvador, M.D.: Influence of microalloying elements on recrystallization texture of warm-rolled interstitial free steels. Mater. Trans. **51**(4), 625–634 (2010)
17. Motohashi, Y., Ryukhtin, V., Takaaki, S., Saroun, J.: Influence of flat cavity formation on stress vs. strain and strain rate relations of superplastic deformation in 3Y–TZP. Mater. Trans. **51**(3), 567–573 (2010)
18. Pero-Sanz, J.A.: Steels: Physical Metallurgy. Selection and Design. CIE–Dossat 2000, Madrid (2004) (in Spanish)
19. Furuhara, T., Maki, T.: Grain boundary engineering for superplasticity in steels. J. Mater. Sci. **40**, 919–926 (2005)
20. Vervynckt, S., Verbeken, K., López, B., Jonas, J.J.: Modern HSLA steel and role of non-recrystallisation temperature. Int. Mater. Rev. **57**, 187–207 (2012)
21. Pero-Sanz, J.A., Sancho, J.P., Verdeja, J.I., Verdeja, L.F.: Ferritic grain size: an ignored factor, in fact, in the failure analysis of the sinking of a famous ship. DYNA **174**, 156–161 (2012)